

# Candidates for non-pulsating stars located in the Cepheid instability strip in the Large Magellanic Cloud based on Strömgren photometry

Weronika Narloch,<sup>1,2,3\*</sup> G. Pietrzynski,<sup>1,3</sup> Z. Kołaczkowski,<sup>3</sup> R. Smolec,<sup>3</sup> M. Górski,<sup>1,2</sup> M. Kubiak,<sup>5</sup> A. Udalski,<sup>5</sup> I. Soszyński,<sup>5</sup> D. Graczyk,<sup>1,2,4</sup> W. Gieren,<sup>1,2</sup> P. Karczmarek,<sup>5</sup> B. Zgirski,<sup>3</sup> P. Wielgórski,<sup>3</sup> K. Suchomska,<sup>5</sup> B. Pilecki,<sup>3</sup> M. Taormina,<sup>3</sup> M. Kałuszyński<sup>3</sup>

<sup>1</sup>Universidad de Concepción, Departamento de Astronomía, Casilla 160-C, Concepción, Chile  
<sup>2</sup>Millennium Institute of Astrophysics, Santiago, Chile  
<sup>3</sup>Nicolaus Copernicus Astronomical Center, Polish Academy of Sciences, Bartycka 18, 00-716 Warsaw, Poland  
<sup>4</sup>Nicolaus Copernicus Astronomical Center, Polish Academy of Sciences, Rabańska 8, 87 - 100 Toruń, Poland  
<sup>5</sup>Warsaw University Observatory, Al. Ujazdowskie 4, 00-478 Warsaw, Poland

Accepted XXX. Received YYY; in original form ZZZ

## ABSTRACT

We present candidates for non-pulsating stars lying in the classical Cepheid instability strip based on OGLE photometric maps combined with Strömgren photometry obtained with the 4.1-m SOAR telescope, and Gaia DR2 data in four fields in the Large Magellanic Cloud. We selected 19 candidates in total. After analysis of their light curves from OGLE surveys we found that all these stars appear to be photometrically stable at the level of a few mmag. Our results show that non-pulsating stars might constitute to about 21% – 30% of the whole sample of giant stars located in the classical instability strip. Furthermore, we identified potential candidates for classical Cepheids with hot companions based on their Strömgren colours.

**Key words:** LMC – Strömgren filters – Cepheids

## 1 INTRODUCTION

The instability strip (IS) is a region on the Herzsprung-Russell (HR) diagram occupied by different classes of pulsating variables (Cox 1974; Gautschy&Saio 1996), but a number of early photometric studies showed that significant fraction of stars lying in the Cepheid region of the IS are photometrically stable at the level of tens of mmag (e.g. Fernie&Hube 1971; Schmidt 1972; Percy et al. 1979). Butler (1998) studied 15 such stars lying in or close to IS of Cepheids using photometry and spectroscopy, and showed that most of them indicate, in fact, a variety of behavior. Only four stars did not show any variability on a specified level, for rest of them periodograms of Doppler velocities demonstrated multiple peaks. The author argued that the observed variability might be caused by orbiting planetary mass companions, rotational modulation of surface features or nonradial pulsations. He also reported larger chromospheric activity in the non-Cepheids, but did not explain why the two classes of stars differ.

Guzik et al. (2013) used *Kepler* data to examine light curves of a sample of 633 stars that were likely to be in or near the IS of  $\delta$  Sct and  $\gamma$  Dor stars, among which they found 359 *stable* stars. Six of the non-pulsating objects were lying within the IS boundaries. The authors argue that uncertainties on the temperatures and gravities for their *stable* objects may mean that some of the stars may move into or out of the IS regions. If these uncertainties are random and not systematic then about 2% of their sample would be within the IS boundaries. Later, Guzik et al. (2015) presented results for additional 2137 stars among which they found another 34 such objects (1.6%). As possible explanations of the lack of pulsations the authors of these papers mention: pulsation in different frequencies hard to detect, turning off pulsations due to various mechanisms or simply an error in determination of  $\log g$  or  $T_{\text{eff}}$ . Also Murphy et al. (2015) found stars in the  $\delta$  Sct IS that do not pulsate in p modes at the 50- $\mu$ mag limit, using *Kepler* data. The authors investigated the possibility that the non-pulsators inside the IS could be unresolved binary systems, having components that both lie outside the IS. That interpretation would explain most of the analyzed systems, except one star which resided in the center of the IS.

\* E-mail: wnarloch@astro-udec.cl (WN)

Gieren et al. (2015) reported a classical Cepheid in an eclipsing binary system OGLE-LMC-CEP-4506, in which the secondary component turned out to be a non-pulsating red giant residing in the center of the classical IS, which was later confirmed by Pilecki et al. (2018). Both stars of this system have similar masses, radii and colours, with the Cepheid being more evolutionary advanced. Within uncertainties both stars have the same effective temperature ( $T_2/T_1 = 0.99$ ), and only slightly different luminosities ( $L_2/L_1 = 0.83$ ). The orbit of the binary is highly eccentric and the orbital period is long – about 4.2 years. According to the results of the analysis of six similar systems presented in Pilecki et al. (2018), all other six stars residing in the IS pulsate (including a system composed of two Cepheids) and there is no pulsating star outside the IS.

Furthermore, recently Rozycka et al. (2018) confirmed that variable V4 in the globular cluster M10 (NGC6254) suspected to be RR Lyr-type star (Clement 2001, 2017 edition)<sup>1</sup> is in fact constant. Still, on the base of its proper motion (PM) and distance from the cluster center, the star is a member of M10, so its position on the colour-magnitude diagram (CMD), inside the IS, is not a coincidence.

These few examples show that non-pulsating stars in the IS not only exist but are in fact not so rare. That raises the questions: how many such stars are in the IS? Is it a significant number or just isolated cases? In this work we try to find the answers to these questions using for our purposes images of the Large Magellanic Cloud (LMC) taken in Strömgren filters. The Strömgren photometric system (*uvby*) is a four-colour medium-band photometric system (plus H $\beta$  filters) used for stellar classification (Crawford 1987). The *y* filter is well correlated with the *V*-band from Johnson-Cousins filters; colour (*b* – *y*) determines well temperatures of stars, as well as interstellar reddening; index *m1* = (*v* – *b*) – (*b* – *y*) is sensitive to stellar metallicity and *c1* = (*u* – *v*) – (*v* – *b*) to the surface gravity. All these features make this photometric system useful when it comes to selection of stars of a given type.

The next important questions to answer in the follow-up work will be: what is the nature of these objects? What might be possible causes of the lack of pulsations in these stars? One of the potential reasons worth to consider is the existence of strange modes (large *l* number) which would not cause the changes in light curve but would affect the spectra lines of stars by broadening them. This is still a challenge for the theory of pulsations which does not provide a clear explanation for such situation. Observational premises for this phenomenon would be very valuable to supplement and develop theoretical knowledge.

The paper is organized as follows: in Section 2 we describe our data and reduction procedure, in Section 3 we present the method of selecting candidates for non-pulsating stars lying in the IS, Section 4 summarizes our search for variability in the OGLE light curves of the selected candidates and provide a short discussion on our search, and finally Section 5 contains a brief summary.

<sup>1</sup> Webpage: <http://www.astro.utoronto.ca/~cclement/cat/C1654m040>

**Table 1.** Information about analyzed fields. Field - number of the field in the LMC; RA, DEC - equatorial coordinates of the center of the fields; E(B-V) - calculated reddening value.

Field	RA J2000.0	DEC J2000.0	E(B-V) [mag]
1	05:17:07.850	-69:21:35.500	0.1114
2	05:18:02.196	-69:43:35.904	0.08795
3	05:18:17.726	-69:36:57.215	0.08590
4	05:28:50.495	-69:51:44.017	0.09976

## 2 OBSERVATIONS AND DATA REDUCTION

Single images of four fields in the LMC (numbered 1, 2, 3 and 4) analyzed in this paper were collected within the ARAUCARIA project (Gieren et al. 2005) during one night on December 17<sup>th</sup> 2008 (programme ID: SO2008B-0917, PI: Pietrzynski). The fields were chosen so that they contained a relatively large amount of Cepheids. Observations in four Strömgren filters *u*, *v*, *b* and *y* were obtained using the 4.1-m Southern Astrophysical Research Telescope (SOAR) on Cerro Pachón in Chile, equipped with SOAR Optical Imager (SOI). SOI is an imager using a mini-mosaic of two E2V 2k × 4k CCDs with a total field of view covering 5.26 × 5.26 arcmin<sup>2</sup> at a pixel scale of 0.077 arcsec/pixel. We used pixel binning which resulted in a pixel scale of 0.154 arcsec/pixel. Each chip was read out by two amplifiers. Table 1 summarizes RA and DEC of the analyzed fields. The average seeing for each filter was 0.81 arcsec for *y* and *b*, 0.89 arcsec for *v* and 0.91 arcsec for *u*.

Images were calibrated with standard bias subtraction and flatfield correction for each amplifier separately. In the next step, profile photometry was performed with standard DAOPHOT/ALLSTAR package (Stetson 1987) assuming a Gaussian function with spatial variability to define point spread function (PSF). Additionally, to reduce the effect of PSF variability, images from each amplifier were divided into smaller, overlapping subframes. Master list for each subframe was obtained iteratively, gradually decreasing the detection threshold. In the last iteration images were examined by eye to add manually stars omitted in the automatic procedure. In the end, aperture corrections, calculated with DAOGROW package (Stetson 1990), were applied to each subframe and instrumental CMDs were constructed. The average errors of our photometry were 0.02 mag in (*b* – *y*), 0.03 mag in *m1* and 0.04 mag in *c1* for stars with brightness *V* < 19 mag.

The completeness of our photometry was checked with DAOPHOT package by adding one hundred artificial stars to each subframe in filter *y*. Twenty such images were produced in each subfield of each field. Next, the same set of stars was added to the images in the other three filters, so that in every filter were checked the retrieving rates of the same stars. Statistics in all four fields are similar. For stars with brightness 13 < *V* < 18 mag the completeness is at the level of about 100% in all four filters. Stars brighter than 13<sup>th</sup> magnitude are often overexposed which results in decrease of completeness to the level of about 70% but no lower than 56% in all filters. Completeness of stars from magnitude bin of (18, 19) is still over 90% in *y*, *b* and *v* but slightly lower in *u*. In the range (19, 20) it decreases to about 87% in *y*, 82% in

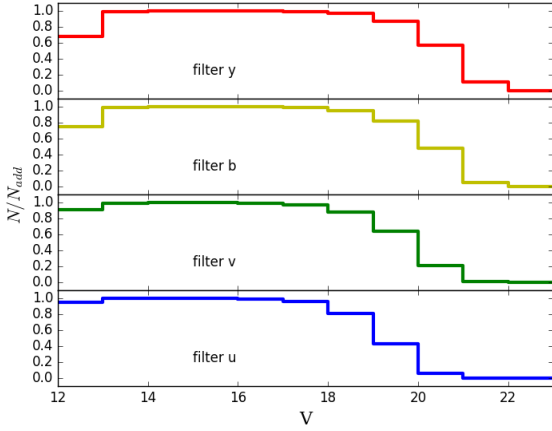


**Figure 1.** Completeness of our photometry in four Strömgren filters.

*b*, 64% in *v* and only 43% in *u*. Completeness for stars from magnitude range (20, 21) drops significantly to about 57% in *y*, 48% in *b*, 21% in *v* and only about 6% in *u*. In a bin (21, 22), completeness is only about 10% and 5% for filters *y* and *b*, respectively. For stars fainter than 22 magnitude it is practically zero in all filters. Figure 1 presents completeness in four Strömgren filters.

Magnitude *y*, colour  $(b - y)$  and indices  $c1$  and  $m1$  were standarized for each chip individually based on standard stars observed during the same photometric night. From 14 stars observed in 10 fields on chip 1, 12 stars were used for photometric calibration of *y*,  $(b - y)$  and  $m1$  and 8 to calibrate  $c1$ . From 10 stars observed in 10 fields on chip 2, 9 stars were used for photometric calibration of *y* and all 10 to calibrate  $(b - y)$ ,  $m1$  and  $c1$ . Standard values were taken from the Paunzen (2015) catalog. The following transformations, normalized to 1 second, were used for chip 1:

$$y_i = (1.185 \pm 0.033) + (0.996 \pm 0.003) \cdot V - (0.024 \pm 0.019) \cdot (b - y)_s + (0.104 \pm 0.012) \cdot X' \quad (1)$$

$$(b - y)_i = (0.059 \pm 0.007) + (0.973 \pm 0.016) \cdot (b - y)_s + (0.066 \pm 0.012) \cdot X' \quad (2)$$

$$m1_i = (0.327 \pm 0.006) + (0.904 \pm 0.027) \cdot m1_s + (0.189 \pm 0.024) \cdot (b - y)_s + (0.051 \pm 0.010) \cdot X' \quad (3)$$

$$c1_i = -(0.558 \pm 0.073) + (1.139 \pm 0.078) \cdot c1_s + (0.014 \pm 0.087) \cdot (b - y)_s + (0.142 \pm 0.024) \cdot X' \quad (4)$$

and chip 2:

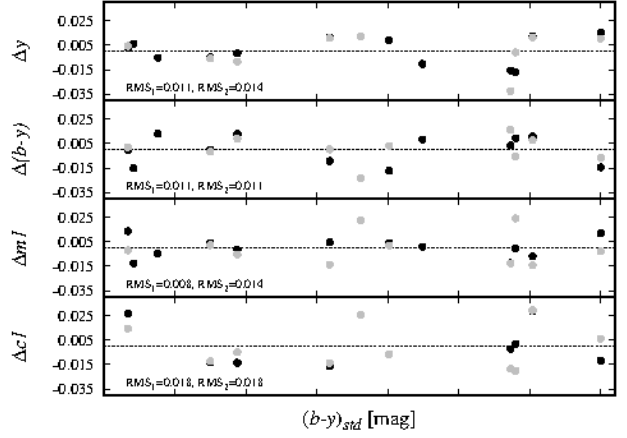


**Figure 2.** Residua and *rms* of photometric calibration to standard system. Black and grey points mark residua for chip 1 and 2, respectively.

$$y_i = (1.176 \pm 0.216) + (0.998 \pm 0.021) \cdot V - (0.002 \pm 0.037) \cdot (b - y)_s + (0.113 \pm 0.020) \cdot X' \quad (5)$$

$$(b - y)_i = (0.051 \pm 0.009) + (0.973 \pm 0.019) \cdot (b - y)_s + (0.054 \pm 0.012) \cdot X' \quad (6)$$

$$m1_i = (0.322 \pm 0.012) + (0.929 \pm 0.057) \cdot m1_s + (0.128 \pm 0.053) \cdot (b - y)_s + (0.065 \pm 0.017) \cdot X' \quad (7)$$

$$c1_i = -(0.641 \pm 0.052) + (1.116 \pm 0.058) \cdot c1_s + (0.018 \pm 0.067) \cdot (b - y)_s + (0.136 \pm 0.022) \cdot X', \quad (8)$$

where  $X' = X - 1.25$  is an airmass;  $y_i$ ,  $(b - y)_i$ ,  $m1_i$  and  $c1_i$  are instrumental and  $V$ ,  $(b - y)_s$ ,  $m1_s$  and  $c1_s$  are standard magnitudes and indices, respectively. Figure 2 presents residua and *rms* of applied transformations for both chips. To check the internal consistency of our transformations between chips we fitted the Paczyński profile (Paczyński&Stanek 1998) to the histogram of red clump (RC) from chip 1 and 2, and found the center of the pick of the distribution. In the equation 9 of the following form (Górski et al. 2018):

$$n(k) = a + b(k - k_{RC}) + c(k - k_{RC})^2 + \frac{N_{RC}}{\sigma_{RC} \sqrt{2\pi}} \exp\left(-\frac{(k - k_{RC})^2}{2\sigma_{RC}^2}\right) \quad (9)$$

the Gaussian component represents a fit to the RC itself and two other terms describe the background distribution of the red giant stars.  $k$  state for the colour  $(b - y)$ ,  $k_{RC}$  is the mean colour of the RC stars,  $\sigma_{RC}$  the spread of the RC stars colour and  $N_{RC}$  a number of RC stars. The shift in colour between RC from both chips in all four fields was less than 0.02 mag, which is an acceptable difference.

Our final list of stars contains 26291 objects measured to a limiting magnitude of about 21.5 mag in all four filters simultaneously.

### 3 SELECTION OF CANDIDATES

In the first step of the selection of candidates for non-pulsating stars residing in the classical IS of Cepheids in the LMC we determined empirical boundaries of the IS. For this we used the photometry of over 3200 Cepheids from the LMC gathered in the OGLE Collection of Variable Stars and having measurements in both  $V$  and  $I$  filters. The position of stars in the CMD is affected by reddening caused by the interstellar extinction along the line of sight. To correct for this effect we used the reddening values calculated for each field with Cepheids based on the colour of the red clump (Górski et al. 2018, Górska et al. 2019, submitted). Its true colour was determined in 20 fields containing late type eclipsing binaries with reddening values calculated in Graczyk et al. (2018) based on calibration between the equivalent width of the interstellar absorption Na I D1 line and the reddening. The uncertainties of the reddening values in a given field consist of the adopted true colour of the red clump and statistical error of apparent colour measurements where the latter is dominant and are  $\sigma E(B-V) = 0.022$  mag. The details of this calculation will be presented in Górska et al. (2019, submitted). Next, in the overlapping magnitude bins of 0.5 mag wide in  $V$  shifted downwards by 0.1 mag in the range (13.5 – 17.5) mag we calculated histograms of colours and then used step detection technique to find the empirical blue and red edges of the instability strip. Later, we fitted a strait line to these points. This way, we got rather conservative empirical position of the instability strip of Cepheids in the LMC calculated based on thousands of Cepheids (see Figure 3). Stars that are located within IS, but apparently are non-variable, will be our candidates for non-pulsating stars within classical IS.

In the next step, we downloaded the BVI OGLE photometry (Udalski et al. 2000) for our four fields and identified the Cepheids to later exclude them from the sample of potential candidates for non-pulsating stars. We identified 42 classical Cepheids (Soszyński et al. 2015) and two type-II Cepheids (Soszyński et al. 2018), which gave 44 stars in total, summarized in Table 2 (11, 10, 10 and 13 Cepheids in the fields 1, 2, 3 and 4, respectively) where we also give their Strömgren photometry. From the VI CMD of remaining stars we selected these lying within empirical boundaries calculated in the previous step and being no fainter than the faintest Cepheid ( $V_0 = 17.46$  mag). At this stage, we selected 61 stars in total.

As next, we cross-matched the BVI OGLE photometry of candidates with our Strömgren photometry and plotted two-colour diagram  $c1 - (b - y)$  for identified Cepheids and selected stars (see Fig. 4). Our Strömgren data were dereddened using relations of relative extinctions from Schlegel et al. (1998) and the reddening values in our four fields which are given in Table 1. On the same diagram we plotted theoretical  $c1 - (b - y)$  relations for stars from different luminosity classes (having different surface gravity expressed by  $\log g$ ) from static atmosphere models of Castelli&Kurucz (2004) for metallicity  $[\text{Fe}/\text{H}] = -0.5$  (closest to average metallicity of Cepheids in the LMC). The periods for most of identified classical Cepheids range between  $\approx 0.65$  d to  $\approx 11.2$  d which correspond to  $\log g \approx 2.8$  for F mode or 2.7 for 1O mode and  $\log g \approx 1.5$  for F mode or  $\approx 1.3$  for 1O mode, respectively, where most stars have  $\log g \approx 2.0$  (R. Smolec, priv. comm.).

So we shifted theoretical  $c1 - (b - y)$  relations accordingly in  $(b - y)$  colour by  $-0.05$  mag to match our observations. We then decided to select stars lying between theoretical lines for  $\log g = 1.0$  and  $\log g = 3.0$  to cover wide range of possible values of  $\log g$  of Cepheids. This way, we selected giant stars from the sample of potential candidates for non-pulsating stars obtained in the previous step and reduced their number to 27 stars. This procedure is presented in Fig. 4 where we additionally added a theoretical line for  $\log g = 4.5$  (close to solar value) and marked our dereddened standard main sequence stars. They arrange systematically below Cepheids which proves the potential of  $c1$  Strömgren index in separating stars of different luminosity classes. During the pulsation cycle, the effective temperature and brightness of a Cepheid changes and hence the star performs a loop either in the CMD or  $c1 - (b - y)$  relation. It may even leave the instability strip during some pulsation phases. To illustrate this effect, and to estimate how large the excursion beyond the adopted boundaries can be, we have computed a non-linear Cepheid model with  $M = 4.5 M_\odot$ ,  $L = 1784 L_\odot$ ,  $[\text{Fe}/\text{H}] = -0.3$  dex (where convective parameters were a set B adopted by Baranowski et al. (2009), see their tab. 3). The model pulsates in the radial fundamental mode with a period of 5.93 d. The instantaneous effective temperature and gravity (including the dynamic acceleration) were used to compute  $(b - y)_0$  and  $c1_0$  using the static atmosphere models of Castelli&Kurucz (2004). Obviously, using static model atmospheres is not the best approach here, but we just want to estimate the typical extent of the loop followed in the  $c1 - (b - y)$  relation during the pulsation. The result is plotted in Fig. 4 (yellow line). Symbol (yellow square) inside the loop corresponds to the parameters of the equilibrium model.

As a separate test, we downloaded parallaxes and PMs for selected candidates from Gaia DR2 catalog (Gaia Collaboration et al. 2016, 2018b). Fig. 5 presents the Vector Point Diagram (VPD) for our candidates. One star with high proper motion is not shown in the diagram. From the stars we selected those with PMs within a box of  $\pm 1$  mas/yr around the PM of the LMC given by van der Marel&Sahlmann (2016) (marked with black dashed line in Fig. 5). In the end, we were left with 19 candidates in total (3 in field 1, 4 in field 2, 7 in field 3 and 5 in field 4). Remaining stars are most probably giant stars from our galaxy. Table 4 summarizes selected objects.

The result of our selection is presented in Fig. 6, where are marked candidates for non-pulsating stars as well as identified Cepheids. On the other hand, Fig. 7 shows the candidates and Cepheids in the Strömgren CMD which is an independent check of the reliability of our selection procedure. Candidates selected from OGLE CMD should fall into IS also in Strömgren CMD. To check if that is the case, we tranformed the IS boundaries from OGLE CMD into Strömgren CMD using 2nd order polynomial of the form  $(b - y)_0 = 0.0965464(V - I)_0^2 + 0.493749(V - I)_0 - 0.0028315$  (marked in Fig. 7 with dashed blue and red lines). Most of the candidates fit very well into IS region showing that either selection from the OGLE CMD or Strömgren CMD would classify them as non-pulsating stars in the classical IS. However, few stars lie beyond the IS egdes. This might be the effect of approximated transformation of the IS or possible blending of candidates in either OGLE or Strömgren CMD. Also, most of identified Cepheids fit very well in the

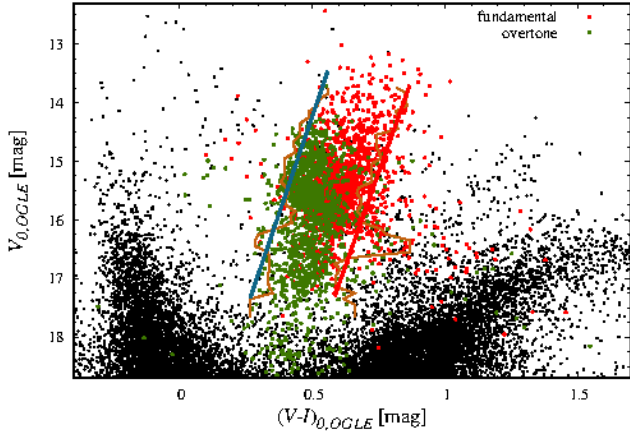


**Figure 3.** Dereddened OGLE CMD for stars brighter than 19 mag from our four fields in the LMC. Red and green points mark fundamental and overtone Cepheids from OGLE Collection of Variable Stars, respectively. Orange curves show the result of applying step detection technique. Strait blue and red lines are fitted to data from previous step and represent adopted borders of empirical IS for classical Cepheids from LMC.

approximated IS, except few, which however is not surprising, since their position on the Strömgren CMD is based on a single colour measurement. As it was already mentioned in previous paragraph, the Cepheids perform a loop in CMD when they change their effective temperature and brightness during its pulsation cycle and in particular phases can go beyond the IS boundaries. In Fig. 7 we marked the results of a non-linear Cepheid model from the  $c_{l0} - (b - y)_0$  relation. The horizontal extent of the loop in the CMD exceeds 0.15 mag in  $(b - y)_0$ . The most profounding Cepheids probably are simply caught in a specific phase. The only exception seems star OGLE-LMC-T2CEP-086 from field 2, which is type II Cepheid located rather well beyond the classical IS. Type II Cepheids are characterized by different physical parameters however; in particular, they have significantly lower masses, akin to that of RR Lyrae stars. This leads to a wider instability strip at lower luminosities, see Smolec (2016).

#### 4 SELECTED CANDIDATES

We selected 19 candidates for non-pulsating stars lying in the IS based on the OGLE CMD combined with the Strömgren photometry which is about 30% of the whole sample of Cepheids and non-pulsating objects located in the classical IS in the LMC. The confrontation of this result with Strömgren CMD put seven of them under the question which would leave us with about 21%. We analyzed the light curves of the candidates downloaded from OGLE-II database (Szymanski 2005)<sup>2</sup> and nonpublic catalogs of OGLE-III and OGLE-IV surveys to check if we might be able to detect any signs of variability. During analysis we arbitrarily assumed signal-to-noise of 4 as a threshold for reliable detection of significant periodicity in the frequency

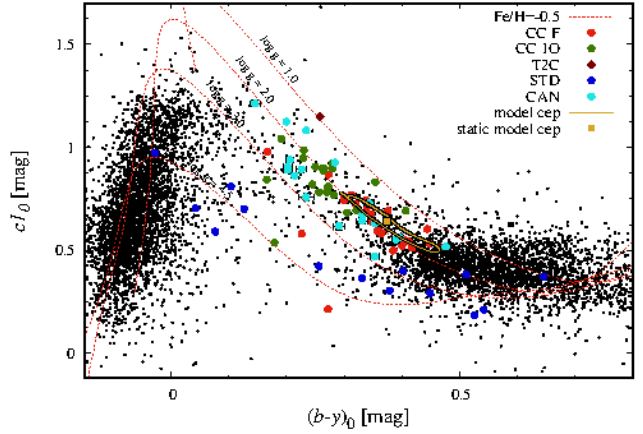


**Figure 4.** Dereddened Strömgren two-colour diagram for stars brighter than 19 mag from our four fields in the LMC. Red and green dots - stars identified in OGLE catalogs as classical Cepheids (CC) pulsating in F and 1O modes, respectively; dark red diamonds - type II Cepheids (T2C); blue dots - standard main sequence stars used for standardization (STD); cyan dots - stars selected from IS as candidates for non-pulsating stars (CAN); red lines - theoretical relations for metallicity  $[Fe/H] = -0.5$  dex; yellow line - model of Cepheid; yellow square - static model of Cepheid.

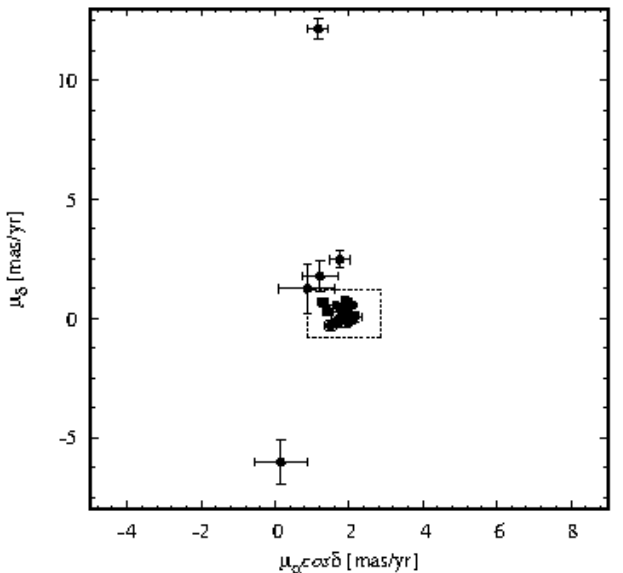


**Figure 5.** Vector Point Diagram for stars selected as candidates for non-pulsating stars in the classical IS based on Gaia DR2 catalog. Black, dashed box encloses stars with proper motions that coincide with the proper motion of the LMC (van der Marel & Sahlmann 2016), and thus belong to this galaxy.

spectrum. For all selected candidates no significant variability was found at the level of a few mmag, so we can assume that these stars are constant at this level of detection.

We shall consider the possibility that our candidates fall into IS because of the blending caused by crowding or because they are physically associated with other stars and

<sup>2</sup> Available at: <http://ogledb.astrowu.edu.pl/~ogle/photdb/>

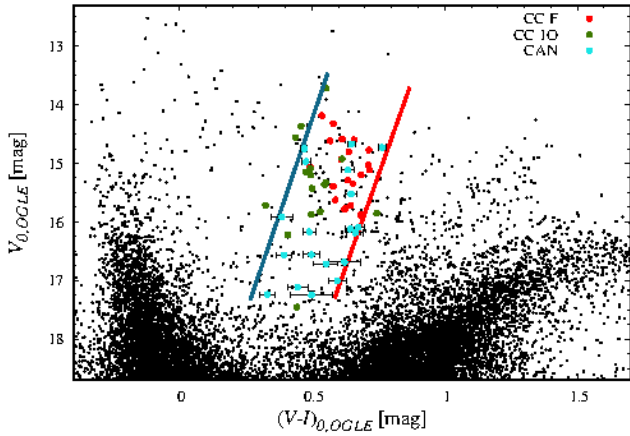


**Figure 6.** Dereddened OGLE CMD with marked Cepheids and candidates for non-pulsating stars in the IS. Red and green dots mark identified classical Cepheids (CC) pulsating in F and 1O modes, respectively. Cyan dots mark candidates for non-pulsating stars (CAN). The blue and red lines present empirical edges of IS.

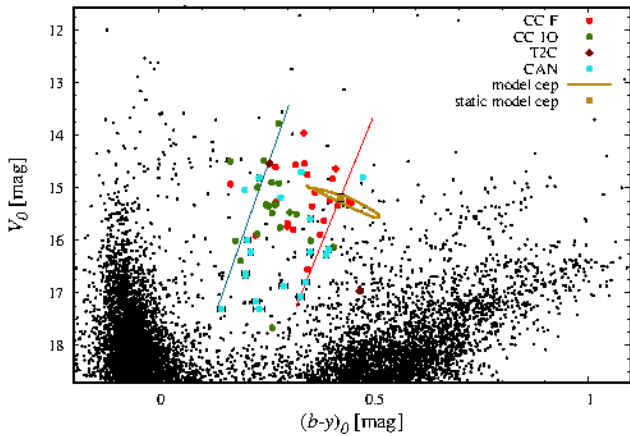


**Figure 7.** Dereddened Strömgren CMD for stars brighter than 19th magnitude. Red and green dots mark stars identified as classical Cepheids (CC) pulsating in F and 1O modes, respectively. Dark red diamonds mark type II Cepheids (T2C). Green dots mark candidates for non-pulsating stars (CAN). Blue and red lines mark the approximate position of the empirical IS determined on the basis of the OGLE cepheid and transformed into Strömgren CMD.

create unresolved binaries or multiple systems, which would change their magnitudes and colours. The second case was discussed in detail by, e.g., [Mochejska et al. \(2000\)](#) where the authors showed that this effect is significant in case of Cepheids. For this example, [Pilecki et al. \(2018\)](#) analyzed Cepheids in eclipsing binaries in the LMC. They studied seven such systems where one was composed of two classical Cepheids, four were binaries composed of classical Cepheid and constant star and one with a type II Cepheid and constant star. The authors derived precise physical stellar parameters for all components of the systems. This is too small sample of stars to conclude any typical features of binaries

with Cepheids but it gives us a concept of how big may be the change of colour of a Cepheid with a companion star. The smallest  $(V - I)$  colour difference of a single classical Cepheids relative to the colour of the binary was 0.005 mag and the biggest 0.19 mag which correspond to  $\approx 0.003$  and  $\approx 0.1$  mag, respectively, in Strömgren system. The exceptionally large change of colour had a system with type II Cepheid which was about 0.7 mag ( $\Delta(b - y) \approx 0.4$  mag). Interestingly, in all systems no third light was detected. Thus, if the colour difference of a single Cepheids and their binaries can be so significant that they can fall out from IS then also the opposite situation can take place when a star originally lying outside IS could fall into it. In the extreme case, all of our candidates might be blends. Unfortunately, we need the spectroscopy in order to investigate the nature of the candidates. At this stage, we are not able to resolve this matter. However, we can estimate the effect of crowding on our selected stars based on our Strömgren data.

In order to estimate what might be the influence of the crowding on our candidates, we performed a series of simulations. In each subfield of our four fields we take a catalog with Strömgren photometry and draw a subsample of 100 stars with magnitudes measured in all four filters simultaneously. Next, randomly we draw x and y coordinates in pixels from a uniform distribution from the range of the image size. In DAOPHOT package we use task *add* to add created lists of stars in a specific filter to the image in this filter. We repeat this procedure 100 times for each subfield of a given field. Then, we perform the photometry on images with added stars and calculate the resulting colours. Subsequently, we calculate the differences between the actual colours and new colours of added stars. From the latter we can estimate what is the influence of the crowding effect in all our fields. The four considered fields are located in the bar of the LMC and have similar star density. This is reflected in statistics of crowding effect for all fields, which is similar. On average 53% of added stars from the vicinity of the IS changed their  $(b - y)$  colour by more than 0.01 mag, 11% by more than 0.05 mag and only 5% by more than 0.1 mag. Most of the candidates reside relatively deep in the IS. They would have to change their colours significantly to enter IS as a blend and this is very unlikely. On the other hand, there is more than 50% chance that candidates lying close the IS edges failed into it as a consequence of blending due to crowding. There are seven such stars in OGLE CMD. Comparison of two CMDs (OGLE and Strömgren) also shows that over one third of stars could be blended due to crowding and because of that entered IS. That still leave us with 12 candidates for non-pulsating stars which account for 21.4% of the whole sample of giant stars in the IS region.

#### 4.1 Cepheids in analyzed fields

In Fig. 8 we plotted relation  $(u - b) - \log P$  for 41 classical Cepheids identified in our fields ([Soszyński et al. 2015](#)). Most of the stars lie in the bottom of the figure creating a linear relation, scatter of which is a consequence of having only one random measurement of the brightness. Two stars which have the largest colour differences clearly stand out from that relation. Two others are questionable. These are very likely binaries with hot main sequence component,

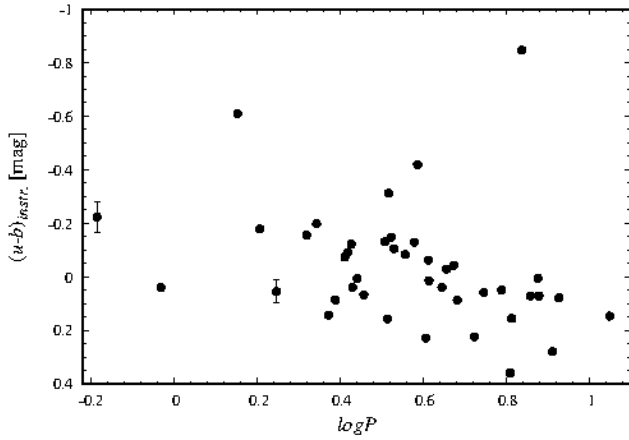


**Figure 8.**  $(u-b) - \log P$  relation for classical Cepheids identified in the four fields in the LMC.

bright in  $u$ -band. Further spectroscopic observations would be required to confirm the binary nature of those systems.

## 5 CONCLUSIONS

Based on OGLE photometric maps combined with Strömgren photometry and Gaia DR2 data for four fields in the LMC we found 19 candidates for non-pulsating stars located in empirical instability strip. An analysis of their light curves downloaded from OGLE surveys confirmed that they are stable at the level of a few of mmag. Our results show that between about 21% to 30% of LMC giants located in the IS might not pulsate. More observations will be required for further investigation of the candidates, in order to find any signs of variability indicating kinds of behavior other than classical pulsations, e.g., nonradial pulsation or binarity (where both components of the system lie in fact outside the IS).

The relation  $(u-b) - \log P$  plotted for classical Cepheids identified in the fields gave us two potential candidates for binary Cepheids with hot companions and two other are questionable. These systems might be interesting for further follow up spectroscopic observations to confirm these suspicions.

In this work, we showed that the number of potential non-pulsating stars in the classical IS of Cepheids is a non-zero number and its upper limit suggests that it might be even significant percentage of giants in the IS. The follow up spectroscopic studies shall revise this conclusion, but basing on photometry we show it is very likely that non-pulsating stars exist in the IS. The great potential of multiband photometry combined with spectroscopy and Gaia proper motions could provide information about the nature of these mysterious objects.

## ACKNOWLEDGEMENTS

We thank anonymous reviewer for comments which helped to improve original manuscript.

W.N. thanks prof. Andrzej Soltan for a fruitful discussion about statistics.

We thank the staff of Cerro Tololo Observatory for a support during the observations.

W.N., G.P., Z.K., R.S. and M.G. were partly supported by the grant MAESTRO 2012/06/A/ST9/00269 from the Polish National Science Center.

B.P. acknowledges financial support for this work from the Polish National Science Center grant SONATA 2014/15/D/ST9/02248.

Authors were also partially supported by the grant IDEAS PLUS IdP II 2015 0002 64 of the Polish Ministry of Science and Higher Education.

The OGLE project received funding from the Polish National Science Centre grant MAESTRO no. 2014/14/A/ST9/00121

The research leading to these results has received funding from the European Research Council (ERC) under the European Unions Horizon 2020 research and innovation program (grant agreement No. 695099). W.N., W.G., M.G. and D.G. gratefully acknowledge financial support for this work from the Millennium Institute of Astrophysics (MAS) of the Iniciativa Científica Milenio del Ministerio de Economía, Fomento y Turismo de Chile, project IC120009. We (W.G., G.P., and D.G.) also very gratefully acknowledge financial support for this work from the BASAL Centro de Astrofísica y Tecnologías Afines (CATA) AFB-170002.

This work has made use of data from the European Space Agency (ESA) mission *Gaia* (<https://www.cosmos.esa.int/gaia>), processed by the *Gaia* Data Processing and Analysis Consortium (DPAC, <https://www.cosmos.esa.int/web/gaia/dpac/consortium>). Funding for the DPAC has been provided by national institutions, in particular the institutions participating in the *Gaia* Multilateral Agreement.

## REFERENCES

Baranowski R., Smolec R., Dimitrov W., Kwiatkowski T., Schwarzenberg-Czerny A., Bartczak P., Fagas M., Borczyk W., Kamiński K., Moskalik P., Ratajczak R., Rożek A., 2009, MNRAS, 396, 2194

Butler R. P., 1998, ApJ, 494, 342

Castelli F., Kurucz R. L., 2004, astro-ph, 5087

Clement C. M., Muzzin A., Dufton Q., Ponnampalam T., Wang J., Burford J., Richardson A., Rosebery T., Rowe J., Hogg H. S., 2001, AJ, 122, 2587

Cox J. P., 1974, Rep. Prog. Phys., 37, 563

Crawford D. L., 1987, ngsr. symp., 345

Fernie J. D., Hube J. O., 1971, ApJ, 168, 437

Gaia Collaboration et al., 2016, The Gaia mission. A&A 595, pp. A1

Gaia Collaboration, Brown A. G. A., Vallenari A., Prusti T., de Bruijne J. H. J., Babusiaux C., Bailer-Jones C. A. L., 2018b, Gaia Data Release 2. Summary of the contents and survey properties. ArXiv e-prints:

Gautschy A., Saio H., 1996, Ann. Rev. Astron. Astroph. 34, 551

Gieren W., Pietrzynski G., Bresolin F., Kudritzki R. P., Minniti D., Urbaneja M., Soszynski I., Storm J., Fouque P., Bono G., Walker A., Garcia J., 2005, The Messenger, 121, 23

Gieren W., Pilecki B., Pietrzynski G., Graczyk D., Udalski A., Soszynski I., Thompson I. B., Prada Moroni P. G., Smolec R., Konorski P., Górski M., Karczmarek P., Suchomska K.,

**Table 2.** Stars identified as Cepheids in OGLE catalogs from four fields in the LMC. OGLE - name of the Cepheid in OGLE catalogs (OGLE-LMC-CEP-NNNN, OGLE-LMC-T2CEP-NNN); RA, DEC - equatorial coordinates in degrees; field - name of the field in the LMC; V - V-band magnitude in Johnson-Cousin system from SOAR;  $(b - y)$  - Strömgren colour;  $m1$  -  $m1$  indicator;  $c1$  -  $c1$  indicator; type,mode - identified type and mode of the star (CC - classical Cepheid, T2C - type-II Cepheid).

OGLE	RA	DEC	field	$V_S$ [mag]	$(b - y)$ [mag]	$m1$ [mag]	$c1$ [mag]	P [d]	type,mode
	J2000.0	J2000.0							
1454	79.16290	-69.36194	1	16.496 ± 0.004	0.493 ± 0.006	0.223 ± 0.010	0.713 ± 0.010	2.8663497(53)	CC,1O
1460	79.21088	-69.32492	1	14.864 ± 0.002	0.252 ± 0.003	0.160 ± 0.005	0.863 ± 0.005	3.8617970(67)	CC,1O
1461	79.21956	-69.36780	1	15.995 ± 0.004	0.471 ± 0.005	0.307 ± 0.008	0.519 ± 0.008	4.7178165(47)	CC,F
1463	79.22900	-69.33071	1	14.905 ± 0.002	0.425 ± 0.003	0.262 ± 0.005	0.727 ± 0.005	7.5282566(85)	CC,F
1466	79.24441	-69.39396	1	15.456 ± 0.003	0.450 ± 0.004	0.332 ± 0.007	0.602 ± 0.007	6.1535625(125)	CC,F
1468	79.24965	-69.33508	1	16.163 ± 0.004	0.399 ± 0.006	0.209 ± 0.010	0.790 ± 0.010	3.6069822(48)	CC,F
1471	79.25756	-69.36755	1	18.034 ± 0.018	0.350 ± 0.020	0.120 ± 0.038	0.908 ± 0.082	0.6523943(8)	CC,1O/2O
1479	79.29086	-69.34830	1	16.246 ± 0.004	0.315 ± 0.006	0.192 ± 0.009	0.968 ± 0.045	1.7645509(20)	CC,1O
3832	79.34182	-69.33540	1	14.324 ± 0.004	0.424 ± 0.006	0.232 ± 0.011	0.762 ± 0.016	11.2127522(930)	CC,F
1490	79.35307	-69.34935	1	15.008 ± 0.002	0.498 ± 0.004	0.336 ± 0.007	0.562 ± 0.007	8.1702063(80)	CC,F
1491	79.36054	-69.33521	1	14.854 ± 0.003	0.331 ± 0.004	0.243 ± 0.007	0.840 ± 0.008	4.4205628(154)	CC,1O
1499	79.41005	-69.75534	2	15.522 ± 0.004	0.468 ± 0.005	0.346 ± 0.017	0.537 ± 0.030	5.5756990(40)	CC,F
1500	79.41714	-69.69831	2	15.801 ± 0.003	0.389 ± 0.004	0.238 ± 0.007	0.711 ± 0.007	2.6768609(36)	CC,1O
1502	79.42158	-69.69052	2	15.969 ± 0.003	0.3698 ± 0.004	0.222 ± 0.007	0.758 ± 0.008	3.3402478(37)	CC,F
1509	79.46337	-69.73214	2	14.062 ± 0.002	0.347 ± 0.002	0.218 ± 0.003	0.912 ± 0.004	4.5328125(189)	CC,1O
1512	79.47915	-69.58195	3	15.559 ± 0.004	0.339 ± 0.005	0.214 ± 0.008	0.884 ± 0.009	4.1055073(24)	CC,F
1513	79.48029	-69.76290	2	15.117 ± 0.003	0.473 ± 0.006	0.335 ± 0.012	0.563 ± 0.012	8.4608625(64)	CC,F
1515	79.48530	-69.58140	3	16.189 ± 0.020	0.292 ± 0.022	0.310 ± 0.031	0.596 ± 0.029	3.2864900(16)	CC,F
1517	79.48539	-69.64815	3	15.636 ± 0.004	0.424 ± 0.005	0.358 ± 0.008	0.610 ± 0.008	4.8132991(32)	CC,F
1521	79.50368	-69.73644	2	15.277 ± 0.003	0.298 ± 0.004	0.169 ± 0.005	1.001 ± 0.005	3.2147769(97)	CC,1O
1522	79.50522	-69.62087	3	15.187 ± 0.003	0.329 ± 0.004	0.188 ± 0.005	0.909 ± 0.005	3.3950599(74)	CC,1O
1528	79.52725	-69.65014	3	16.021 ± 0.004	0.365 ± 0.005	0.212 ± 0.008	0.776 ± 0.008	3.7905721(26)	CC,F
1532	79.53612	-69.75633	2	16.844 ± 0.005	0.415 ± 0.006	0.088 ± 0.011	0.691 ± 0.012	2.2056640(7)	CC,F
1533	79.53685	-69.76236	2	15.637 ± 0.003	0.324 ± 0.004	0.252 ± 0.007	0.797 ± 0.007	2.7616841(31)	CC,1O
1536	79.54853	-69.58716	3	16.293 ± 0.005	0.420 ± 0.006	0.079 ± 0.010	0.846 ± 0.010	1.6112568(68)	CC,1O
1537	79.55684	-69.70578	2	15.759 ± 0.003	0.373 ± 0.004	0.271 ± 0.007	0.697 ± 0.007	2.6932881(31)	CC,1O
086	79.57418	-69.72433	2	17.251 ± 0.006	0.536 ± 0.008	0.134 ± 0.015	0.529 ± 0.016	15.8455000(829)	T2C/WVir
1549	79.64756	-69.60096	3	16.297 ± 0.004	0.245 ± 0.006	0.157 ± 0.011	0.552 ± 0.015	1.4226693(14)	CC,1O
1550	79.66199	-69.58794	3	16.173 ± 0.005	0.442 ± 0.007	0.227 ± 0.012	0.707 ± 0.012	3.2677563(18)	CC,F
1551	79.67019	-69.65191	3	16.673 ± 0.005	0.257 ± 0.006	0.181 ± 0.010	1.057 ± 0.010	0.9308301(14)	CC,2O
1553	79.67459	-69.63975	3	15.543 ± 0.003	0.510 ± 0.004	0.307 ± 0.008	0.618 ± 0.012	6.4571732(54)	CC,F
2085	82.09549	-69.86013	4	16.091 ± 0.004	0.359 ± 0.006	0.190 ± 0.010	0.788 ± 0.010	2.0879263(20)	CC,1O
2086	82.09638	-69.86773	4	15.643 ± 0.003	0.347 ± 0.004	0.242 ± 0.007	0.801 ± 0.006	2.5793555(21)	CC,1O
2090	82.12354	-69.87687	4	14.890 ± 0.002	0.396 ± 0.003	0.295 ± 0.005	0.743 ± 0.005	7.2263791(63)	CC,F
2094	82.13316	-69.84842	4	15.081 ± 0.003	0.423 ± 0.004	0.314 ± 0.005	0.659 ± 0.005	7.5701883(155)	CC,F
2099	82.14641	-69.85654	4	14.938 ± 0.002	0.349 ± 0.003	0.165 ± 0.005	0.232 ± 0.005	6.8938013(128)	CC,F
2106	82.18173	-69.83431	4	15.672 ± 0.004	0.494 ± 0.006	0.387 ± 0.011	0.532 ± 0.017	5.2938004(73)	CC,F
2107	82.18535	-69.83482	4	15.657 ± 0.004	0.349 ± 0.006	0.214 ± 0.010	0.826 ± 0.010	2.6243078(37)	CC,1O
2109	82.18951	-69.86858	4	15.630 ± 0.003	0.525 ± 0.004	0.302 ± 0.007	0.551 ± 0.008	6.5179412(38)	CC,F
2112	82.21425	-69.83453	4	15.260 ± 0.004	0.244 ± 0.004	0.215 ± 0.006	0.996 ± 0.005	4.1159516(19)	CC,F
129	82.22751	-69.87808	4	14.864 ± 0.002	0.335 ± 0.003	0.038 ± 0.005	1.166 ± 0.005	62.5089466(237959)	T2C/RVTau
2118	82.26211	-69.89023	4	15.651 ± 0.003	0.327 ± 0.009	0.193 ± 0.017	0.923 ± 0.010	2.4461347(26)	CC,1O
2124	82.30195	-69.89078	4	15.247 ± 0.003	0.357 ± 0.004	0.223 ± 0.007	0.939 ± 0.008	4.0439894(103)	CC,1O
2130	82.33005	-69.83155	4	15.813 ± 0.008	0.341 ± 0.009	0.209 ± 0.022	0.918 ± 0.037	2.3572510(32)	CC,1O

Taormina M., Gallenne A., Storm J., Bono G., Catelan M., Szymański M., Kozłowski S., Pietrukowicz P., Wyrzykowski L., Poleski R., Skowron J., Minniti D., Ulaczyk K., Mróz P., Pawlak M., Nardetto N., 2015, *ApJ*, 815, 28

Górski M., Pietrzyński G., Gieren W., Graczyk D., Suchomska K., Karczmarek P., Cohen R. E., Zgirski B., Wielgórski P., Pilecki B., Taormina M., Kołaczkowski Z., Narloch W., 2018, *AJ*, 156, 278

Graczyk D., Soszyński I., Poleski R., Pietrzyński G., Udalski A., Szymański M. K., Kubiak M., Wyrzykowski L., Ulaczyk K., 2011, *AcA*, 61, 103

Graczyk D., Pietrzyński G., Thompson I. B., Gieren W., Pilecki B., Konorski P., Villanova S., Górska M., Suchomska K., Kar-

czmarek P., Stepień K., Storm J., Taormina M., Kołaczkowski Z., Wielgórski P., Narloch W., Zgirski B., Gallenne A., Os-trowski J., Smolec R., Udalski A., Soszyński I., Kervella P., Nardetto N., Szymański M. K., Wyrzykowski L., Ulaczyk K., Poleski R., Pietrukowicz P., Kozłowski S., Skowron J., Mróz P., 2018, *ApJ*, 860, 1

Guzik J. A., Bradley P. A., Jackiewicz J., Uytterhoeven K., Kinemuchi K., 2013, *Astr.Rev.*, 8:3, 83-107

Guzik J. A., Bradley P. A., Jackiewicz J., Molenda-Zakowicz J., Uytterhoeven K., Kinemuchi K., 2015, arXiv: <https://arxiv.org/pdf/1502.00175.pdf>

Haschke R., Grebel E. K., Duffau S., 2011, *AJ*, 141, 158

Mochejska B. J., Macri L. M., Sasselov D. D., Stanek K. Z., 2000,

**Table 3.** Candidates for non-pulsating stars in the IS from four fields in the LMC. ID - name of the candidate; RA, DEC - equatorial coordinates in degrees; field - number of the field in the LMC;  $V_O$  - OGLE-II magnitude;  $(V - I)_O$  - OGLE-II colour;  $V_S$  - V-band magnitude in Johnson-Cousin system from SOAR;  $(b - y)$  - Strömgren colour;  $m1$  -  $m1$  indicator;  $c1$  -  $c1$  indicator.

ID	RA J2000.0	DEC J2000.0	field	$V_O$ [mag]	$(V - I)_O$ [mag]	$V_S$ [mag]	$(b - y)$ [mag]	$m1$ [mag]	$c1$ [mag]
CAN-01	79.19244	-69.35403	1	15.892 ± 0.019	0.789 ± 0.021	15.958 ± 0.004	0.439 ± 0.006	0.231 ± 0.009	0.653 ± 0.008
CAN-02	79.23039	-69.36134	1	17.607 ± 0.018	0.473 ± 0.027	17.675 ± 0.006	0.231 ± 0.009	0.104 ± 0.016	1.232 ± 0.015
CAN-03	79.32142	-69.38572	1	15.340 ± 0.012	0.619 ± 0.017	15.407 ± 0.003	0.286 ± 0.004	0.155 ± 0.007	1.144 ± 0.007
CAN-04	79.45441	-69.64956	3	17.004 ± 0.040	0.662 ± 0.046	17.160 ± 0.007	0.357 ± 0.010	0.254 ± 0.017	0.632 ± 0.018
CAN-05	79.45741	-69.57179	3	16.848 ± 0.021	0.504 ± 0.030	16.954 ± 0.005	0.268 ± 0.007	0.202 ± 0.012	0.919 ± 0.012
CAN-06	79.46599	-69.75158	2	16.979 ± 0.055	0.734 ± 0.061	17.088 ± 0.006	0.411 ± 0.009	0.035 ± 0.017	0.745 ± 0.018
CAN-07	79.47437	-69.73521	2	16.411 ± 0.017	0.756 ± 0.019	16.518 ± 0.005	0.421 ± 0.007	0.158 ± 0.010	0.486 ± 0.010
CAN-08	79.49751	-69.74904	2	16.207 ± 0.034	0.498 ± 0.040	16.290 ± 0.005	0.274 ± 0.007	0.173 ± 0.010	0.955 ± 0.010
CAN-09	79.50509	-69.63110	3	16.472 ± 0.026	0.772 ± 0.031	16.560 ± 0.005	0.456 ± 0.007	0.239 ± 0.011	0.567 ± 0.012
CAN-10	79.55121	-69.72603	2	15.040 ± 0.008	0.583 ± 0.012	15.100 ± 0.003	0.302 ± 0.004	0.135 ± 0.005	1.097 ± 0.005
CAN-11	79.56479	-69.65368	3	15.400 ± 0.015	0.744 ± 0.022	15.469 ± 0.003	0.350 ± 0.004	0.250 ± 0.007	0.941 ± 0.008
CAN-12	79.56815	-69.65643	3	17.401 ± 0.024	0.556 ± 0.039	17.446 ± 0.007	0.292 ± 0.010	0.180 ± 0.015	0.909 ± 0.016
CAN-13	79.63653	-69.63896	3	16.378 ± 0.019	0.784 ± 0.024	16.463 ± 0.004	0.462 ± 0.006	0.270 ± 0.010	0.577 ± 0.011
CAN-14	79.69809	-69.65521	3	15.014 ± 0.011	0.873 ± 0.014	15.082 ± 0.003	0.542 ± 0.004	0.379 ± 0.008	0.533 ± 0.009
CAN-15	82.09185	-69.86350	4	17.337 ± 0.031	0.722 ± 0.034	17.407 ± 0.006	0.408 ± 0.009	0.170 ± 0.015	0.660 ± 0.016
CAN-16	82.10721	-69.82555	4	16.500 ± 0.017	0.616 ± 0.024	16.557 ± 0.004	0.291 ± 0.006	0.195 ± 0.010	0.881 ± 0.010
CAN-17	82.11237	-69.87718	4	15.002 ± 0.010	0.776 ± 0.014	15.035 ± 0.002	0.409 ± 0.003	0.315 ± 0.005	0.689 ± 0.005
CAN-18	82.14838	-69.84965	4	16.889 ± 0.026	0.625 ± 0.032	16.963 ± 0.005	0.279 ± 0.008	0.099 ± 0.014	0.908 ± 0.012
CAN-19	82.27860	-69.84849	4	17.582 ± 0.072	0.625 ± 0.080	17.639 ± 0.009	0.311 ± 0.013	0.222 ± 0.021	0.776 ± 0.020

**Table 4.** Cross-match of selected candidates for non-pulsating stars in the LMC classical IS with OGLE catalogs: ID - name of the candidate; OGLE-II, OGLE-III, OGLE-IV - name of the candidate in OGLE catalogs.

ID	OGLE-II	OGLE-III	OGLE-IV
CAN-01	LMC_SC8 224920	LMC100.7.17275	LMC503.13.120132
CAN-02	LMC_SC8 225288	LMC100.7.17672	LMC503.13.120383
CAN-03	LMC_SC8 312232	LMC100.7.17331	LMC503.13.36068
CAN-04	LMC_SC7 22149	LMC103.5.30585	LMC503.05.44074
CAN-05	LMC_SC7 38882	LMC103.5.92208	LMC503.13.248
CAN-06	LMC_SC7 14125	LMC103.6.78881	-
CAN-07	LMC_SC7 14162	LMC103.6.78891	LMC503.05.26852
CAN-08	LMC_SC7 14127	LMC103.6.78900	LMC503.05.26808
CAN-09	LMC_SC7 30218	LMC103.5.30386	LMC503.05.43806
CAN-10	LMC_SC7 134320	LMC103.6.78723	-
CAN-11	LMC_SC7 142141	LMC103.5.30256	LMC503.04.109410
CAN-12	LMC_SC7 142382	LMC103.5.47427	LMC503.04.109830
CAN-13	LMC_SC7 142250	LMC103.5.47327	LMC503.04.109565
CAN-14	LMC_SC7 142103	LMC103.5.47191	LMC503.04.109345
CAN-15	LMC_SC3 162486	LMC162.2.117682	-
CAN-16	LMC_SC3 170350	LMC162.3.63638	LMC516.23.68773
CAN-17	LMC_SC3 162131	LMC162.2.136551	LMC516.23.54100
CAN-18	LMC_SC3 170298	LMC162.2.136736	LMC516.23.68723
CAN-19	LMC_SC3 282212	LMC169.7.83593	LMC516.23.68910

AJ, 120, 810  
Murphy S. J., Bedding T. R., Niemczura E., Kurtz D. W., Smalley B., 2015, MNRAS, 447, 3948  
Paczyński B., Stanek K. Z., 1998, ApJ, 494, 219  
Paunzen E., 2015, A&A, 580, A23  
Percy J. R., Baskerville I., Trevorrow D. W., 1979, PASP, 91, 368  
Pilecki B., Gieren W., Pietrzynski G., Thompson I. B., Smolec R., Graczyk D., Taormina M., Udalski A., Storm J., Nardetto N., Gallenne A., Kervella P., Soszyński I., Górska M., Wielgórski P., Suchomska K., Karczmarek P., Zgirski B., 2018, ApJ, 862, 43  
Rozyczka M., Narloch W., Schwarzenberg-Czerny A., Thompson I. B., Poleski R., Pych W., 2018, AcA, 68, 237

Schmidt E. G., 1972, ApJ, 172, 679  
Smolec R., 2016, MNRAS, 456, 3475  
Soszyński I., Udalski A., Szymański M. K., Skowron D., Pietrzynski G., Poleski R., Pietrukowicz P., Skowron J., Mróz P., Kozłowski S., Wyrzykowski Ł., Ulaczyk K., Pawlak M., 2015, AcA, 65, 297  
Soszyński I., Udalski A., Szymański M. K., Wyrzykowski Ł., Ulaczyk K., Poleski R., Pietrukowicz P., Kozłowski S., Skowron D., Skowron J., Mróz P., Rybicki K., Iwanek P., 2018, AcA, 68, 89  
Schlegel D. J., Finkbeiner D. P., Davis M., 1998, ApJ, 500, 525  
Stetson P. B., 1987, PASP, 99, 191  
Stetson P. B., 1990, PASP, 102, 932

Szymanski M. K., 2005, *AcA*, 55, 43  
Udalski A., Szymanski M., Kubiak M., Pietrzynski G., Soszynski  
I., Wozniak P., Zebrun K., 2000, *AcA*, 50, 307  
van der Marel R. P., Sahlmann J., 2016, *ApJ*, 832, L23  
Zebrun K., Soszynski I., Wozniak P. R., Udalski A., Kubiak M.,  
Szymanski M., Pietrzynski G., Szewczyk O., Wyrzykowski L.,  
2001, *AcA*, 51, 317

This paper has been typeset from a *TeX/LaTeX* file prepared by  
the author.